Electromagnetic response of a vortex in layered superconductors

M. Eschrig and J. A. Sauls
Department of Physics & Astronomy, Northwestern University, Evanston, Illinois 60208

D. Rainer
Physikalisches Institut, Universität Bayreuth, D-95440 Bayreuth, Germany

(Received 10 May 1999)

We calculate the response of a vortex core in a layered superconductor to an ac electromagnetic field. In particular we investigate the intermediate clean regime, where the broadening of the vortex core bound states is comparable to or larger than the level spacing. The response of the order parameter, impurity self-energy, and currents are obtained by a self-consistent determination of the distribution functions and the excitation spectrum. The response is dominated by order parameter collective modes coupled to the fermion excitations of the vortex core. At low frequencies this coupling leads to substantially enhanced absorption in the vortex core. [S0163-1829(99)11237-2]

I. INTRODUCTION

Vortex cores play a key role in dissipation processes of superconductors in the Abrikosov phase. Bardeen and Stephen[1] modeled the vortex core as a region of normal metal in which the excitations in the core respond to an electromagnetic field like electrons in the normal metallic state. This is a good approximation for dirty superconductors with a mean free path l much smaller than the coherence length ξ_0. However, in clean superconductors the low-lying excitations in the core are the bound states of Caroli, de Gennes, and Matricon.[2] These excitations have superconducting as well as normal properties. They are the source of circulating supercurrents in the equilibrium vortex core,[3] and they are strongly coupled to the condensate by Andreev's scattering processes.[3,4] Their response to an electromagnetic field is radically different from that of normal electrons. For vortex cores one has two fundamentally different origins of dissipation. One is dissipation by the collective motion of the condensate, and the second is dissipation by transitions between Caroli–de Gennes–Matricon bound states. These processes are coupled because of the strong interaction between the condensate and the bound states, and require a self-consistent treatment of condensate and bound-state dynamics. Earlier calculations of the ac-response neglected this coupling or concentrated on the limit $\omega \to 0$.[5,6] We present a fully self-consistent calculation of the response of the current density in the core to an ac electric field of frequency comparable with the gap frequency $\Delta/\hbar$ or smaller. Our results show that the coupling of condensate and bound-state dynamics is essential for even a qualitative understanding of the low-frequency dynamics of core electrons and the dissipation in the core.

We consider a superconductor with a random distribution of atomic size impurities in a static magnetic field. The applied ac electric field, $\delta \mathbf{E}_0^{\omega}(t) = \delta \mathbf{E}_0 e^{-i\omega t} = -(1/c)\,\partial_t \delta \mathbf{A}^{\omega}(t)$, is linearly polarized in the x direction, and its wavelength is large compared to ξ_0. The impurity scattering rate is assumed to be large enough that the superconductor is outside the superclean limit;[7] i.e., all bound states are broadened by an amount comparable to or larger than the ''minigap,'' Δ^2/E_f.[2] In particular we investigate the intermediate clean regime, $\xi_0 \lesssim l \lesssim (E_f/\Delta)\xi_0$, where we expect the model of a ''normal metal core'' to break down. In this regime we can use the quasiclassical theory,[8] which is a powerful method for studying nonequilibrium superconductivity. This theory describes phenomena on length scales large compared to the microscopic scales (Bohr radius, lattice constant k_f^{-1}, Thomas-Fermi screening length, etc.) and frequencies small compared to the microscopic scales (Fermi energy, plasma frequency, conduction band width, etc.). We use units $\hbar = k_B = 1$, and note that the charge of an electron is $e<0$. The ac frequencies of interest are of the order of the superconducting energy gap, $|\Delta| \sim T_c$, or smaller, and the length scales of interest are the coherence length, $\xi_0 = v_f/2\pi T_c$, and the penetration depth, λ. Hence, our theory requires the conditions $k_f \xi_0 \gg 1$, and $T_c/E_f \ll 1$, where the Fermi wavelength k_f^{-1} and the Fermi energy E_f stand for typical microscopic length and energy scales.

II. THEORETICAL BACKGROUND

The quasiclassical theory is designed for our purposes and is formulated in terms of the quasiclassical Nambu-Keldysh propagator $\check{g}(\mathbf{p}_f, \mathbf{R}; \epsilon, t)$, which is a 4×4 matrix in Nambu-Keldysh space, and a function of position $\mathbf{R}$, time t, energy ϵ, and momenta $\mathbf{p}_f$ on the Fermi surface. For a review of the methods and an introduction to the notation we refer to the article by Larkin and Ovchinnikov.[9] We denote Nambu-Keldysh matrices by a ''check'' accent, and their 2×2 Nambu submatrices of *advanced* (superscript A), *retarded* (superscript R), and Keldysh-type (superscript K) by a ''hat'' accent. In this notation the transport equation and the normalization condition read

$$\left[\left(\epsilon + \frac{e}{c}\mathbf{v}_f \cdot \mathbf{A}\right)\check{\tau}_3 - \check{\Delta}_{mf} - \check{\sigma}_i - \delta\check{v}, \check{g}\right]_{\otimes} + i\mathbf{v}_f \cdot \boldsymbol{\nabla}\check{g} = 0, \quad (1)$$

$$\check{g} \otimes \check{g} = -\pi^2 \check{1}, \quad (2)$$

where $\mathbf{A}(\mathbf{R})$ is the vector potential of the static magnetic field, $\mathbf{B}=\boldsymbol{\nabla}\times\mathbf{A}$, $\check{\Delta}_{mf}(\mathbf{p}_f,\mathbf{R};t)$ is the mean-field order parameter matrix, and $\check{\sigma}_i(\mathbf{p}_f,\mathbf{R};\epsilon,t)$ is the impurity self-energy. The perturbation $\delta\check{v}(\mathbf{p}_f,\mathbf{R};t)$ includes the external electric field and the field of the induced charge fluctuations $\delta\rho(\mathbf{R};t)$. The commutator $[\check{A},\check{B}]_\otimes$ is $\check{A}\otimes\check{B}-\check{B}\otimes\check{A}$, where the noncommutative $\otimes$ product is defined by

$$\check{A}\otimes\check{B}(\epsilon,t)=e^{\frac{i}{2}(\partial_\epsilon^A\partial_t^B-\partial_t^A\partial_\epsilon^B)}\check{A}(\epsilon,t)\check{B}(\epsilon,t). \tag{3}$$

For convenience we work in a gauge where the external electric field is defined by a vector potential $\delta\mathbf{A}^\omega(t)$ and the induced electric field is obtained from the electrochemical potential $\delta\Phi(\mathbf{R};t)$. We consider the limit of large $\kappa=\lambda/\xi_0$, so that we can neglect corrections to the vector potential due to the induced current densities, which are proportional to $1/\kappa^2$. Hence in the Nambu-Keldysh matrix notation the perturbation has the form

$$\delta\check{v}=-\frac{e}{c}\mathbf{v}_f\cdot\delta\mathbf{A}^\omega(t)\check{\tau}_3+e\,\delta\Phi(\mathbf{R};t)\check{1}, \tag{4}$$

and is assumed to be sufficiently small so that it can be treated in linear response theory.

Equations (1)–(4) must be supplemented by self-consistency equations for the order parameter and the impurity self-energy. We use the weak-coupling gap equations

$$\hat{\Delta}_{mf}^{R,A}(\mathbf{R};t)=N_f\mathcal{V}\int_{-\epsilon_c}^{+\epsilon_c}\frac{d\epsilon}{4\pi i}\langle\hat{f}^K(\mathbf{p}_f',\mathbf{R};\epsilon,t)\rangle, \tag{5}$$

$$\hat{\Delta}_{mf}^{K}(\mathbf{R};t)=0, \tag{6}$$

and the impurity self-energy in Born approximation with isotropic scattering,

$$\check{\sigma}_i(\mathbf{R};\epsilon,t)=\frac{1}{2\pi\tau}\langle\check{g}(\mathbf{p}_f',\mathbf{R};\epsilon,t)\rangle. \tag{7}$$

The Nambu matrix $\hat{f}^K$ is the off-diagonal part of $\hat{g}^K$, and the Fermi surface average is defined by

$$\langle\cdots\rangle=\frac{1}{N_f}\int\frac{d^2\mathbf{p}_f'}{(2\pi)^3|\mathbf{v}_f'|}\cdots,\quad N_f=\int\frac{d^2\mathbf{p}_f'}{(2\pi)^3|\mathbf{v}_f'|}. \tag{8}$$

The material parameters that enter the self-consistency equations are the dimensionless pairing interaction $N_f\mathcal{V}$, the impurity scattering lifetime τ, and the Fermi surface data: $\mathbf{p}_f$ (Fermi surface), $\mathbf{v}_f$ (Fermi velocity), and N_f (averaged density of states at the Fermi surface). We eliminate both the magnitude of the pairing interaction and the cutoff in Eq. (5) in favor of the transition temperature T_c.

A. Linear response

In the linear response approximation we split the propagator and the self-energies into an unperturbed part and a term of first order in the perturbation

$$\check{g}=\check{g}_0+\delta\check{g},\quad \check{\Delta}_{mf}=\check{\Delta}_{mf0}+\delta\check{\Delta}_{mf},\quad \check{\sigma}_i=\check{\sigma}_0+\delta\check{\sigma}_i, \tag{9}$$

and expand the transport equation and normalization condition through first order. In zeroth order

$$\left[\left(\epsilon+\frac{e}{c}\mathbf{v}_f\cdot\mathbf{A}\right)\check{\tau}_3-\check{\Delta}_{mf0}-\check{\sigma}_0,\check{g}_0\right]_\otimes+i\mathbf{v}_f\cdot\boldsymbol{\nabla}\check{g}_0=0, \tag{10}$$

$$\check{g}_0\otimes\check{g}_0=-\pi^2\check{1}, \tag{11}$$

and in first order

$$\left[\left(\epsilon+\frac{e}{c}\mathbf{v}_f\cdot\mathbf{A}\right)\check{\tau}_3-\check{\Delta}_{mf0}-\check{\sigma}_0,\delta\check{g}\right]_\otimes+i\mathbf{v}_f\cdot\boldsymbol{\nabla}\delta\check{g}=[\delta\check{\Delta}_{mf}+\delta\check{\sigma}_i+\delta\check{v},\check{g}_0]_\otimes, \tag{12}$$

$$\check{g}_0\otimes\delta\check{g}+\delta\check{g}\otimes\check{g}_0=0. \tag{13}$$

In order to close this system of equations one has to supplement the transport and normalization equations with the zeroth and first order self-consistency equations for the order parameter,

$$\hat{\Delta}_{mf0}^{R,A}(\mathbf{R})=N_f\mathcal{V}\int_{-\epsilon_c}^{+\epsilon_c}\frac{d\epsilon}{4\pi i}\langle\hat{f}_0^K(\mathbf{p}_f',\mathbf{R};\epsilon)\rangle, \tag{14}$$

$$\delta\hat{\Delta}_{mf}^{R,A}(\mathbf{R};t)=N_f\mathcal{V}\int_{-\epsilon_c}^{+\epsilon_c}\frac{d\epsilon}{4\pi i}\langle\delta\hat{f}^K(\mathbf{p}_f',\mathbf{R};\epsilon,t)\rangle, \tag{15}$$

and the impurity self-energy,

$$\check{\sigma}_0(\mathbf{R};\epsilon)=\frac{1}{2\pi\tau}\langle\check{g}_0(\mathbf{p}_f',\mathbf{R};\epsilon)\rangle, \tag{16}$$

$$\delta\check{\sigma}_i(\mathbf{R};\epsilon,t)=\frac{1}{2\pi\tau}\langle\delta\check{g}(\mathbf{p}_f',\mathbf{R};\epsilon,t)\rangle. \tag{17}$$

The self-consistency equations (15) and (17) for the response of the self-energies are equivalent to vertex corrections in the Green's function response theory, and are particularly important in the context of nonequilibrium superconductivity. The self-consistency conditions guarantee that the quasiclassical theory obeys fundamental conservation laws. In particular, Eqs. (16) and (17) imply charge conservation in scattering processes, whereas Eqs. (14) and (15) imply charge conservation in particle-hole conversion processes; any charge which is lost or gained in a particle-hole conversion process is balanced by the corresponding gain or loss of condensate charge. It is the coupled quasiparticle and condensate dynamics which conserves charge in superconductors. Neglect of the dynamics of either component, or use of a nonconserving approximation for the coupling of quasiparticles and collective degrees of freedom leads to unphysical results.

Finally, the electrochemical potential, $\delta\Phi$ is determined by the condition of local charge neutrality,[10] which is a consequence of the long-range of the Coulomb repulsion. The Coulomb energy of a charged region of size ξ_0^3 and typical charge density $eN_f\Delta$ is $\sim\epsilon^2N_f^2\Delta^2\xi_0^5$, which should be compared with the condensation energy $\sim N_f\Delta^2\xi_0^3$. Thus, the cost in Coulomb energy is a factor $(E_f/\Delta)^2$ larger than the condensation energy. This leads to a strong suppression of charge fluctuations, and the condition of local charge neutrality holds to very good accuracy for superconducting phe-‘‘nomena. The formal result for the change in the charge

density in quasiclassical theory to leading order in Δ/E_f is given in terms of the Keldysh propagator $\delta\hat{g}^K$ by[11]

$$\delta\rho^{(1)}(\mathbf{R};t)=\frac{eN_f}{1+F_0^s}\int\frac{d\epsilon}{4\pi i}\langle \mathrm{Tr}\,\delta\hat{g}^K(\mathbf{p}_f',\mathbf{R};\epsilon,t)\rangle - \frac{2e^2N_f}{1+F_0^s}\delta\Phi(\mathbf{R};t), \tag{18}$$

where F_0^s are Landau parameters. From Maxwell's equation $-\boldsymbol{\nabla}^2\delta\Phi-(1/c)\,\partial_t\boldsymbol{\nabla}\cdot\delta\mathbf{A}=4\pi\delta\rho$, it follows that the change in the charge density $\delta\rho(\mathbf{R};t)$ is of order of $(\Delta/E_f)^3$, implying that the leading order contribution vanishes $\delta\rho^{(1)}(\mathbf{R};t)=0$. This is the condition of ''local charge neutrality,''[10] valid through first order in Δ/E_f; it implies a spatially varying electrochemical potential $\delta\Phi$ determined by

$$2e\,\delta\Phi(\mathbf{R};t)=\int\frac{d\epsilon}{4\pi i}\langle \mathrm{Tr}\,\delta\hat{g}^K(\mathbf{p}_f',\mathbf{R};\epsilon,t)\rangle. \tag{19}$$

The small charge density of order $(\Delta/E_f)^3$, which produces this potential, is calculated (in the high-κ limit) from Poisson's equation

$$\delta\rho(\mathbf{R};t)=-\frac{1}{4\pi}\boldsymbol{\nabla}^2\delta\Phi(\mathbf{R};t). \tag{20}$$

Equations (10)–(17) and (19) constitute a complete set of equations for calculating the electromagnetic response of a vortex. The structure of a vortex in equilibrium is obtained from Eqs. (10), (11), (14), and (16), and the linear response of the vortex to the perturbation $\delta\mathbf{A}(\mathbf{R};t)$ follows from Eqs. (12), (13), (15), (17), and (19). In equilibrium the current circulating around the vortex is given by

$$\mathbf{j}_0(\mathbf{R})=eN_f\int\frac{d\epsilon}{4\pi i}\langle\mathbf{v}_f(\mathbf{p}_f')\mathrm{Tr}[\hat{\tau}_3\hat{g}_0^K(\mathbf{p}_f',\mathbf{R};\epsilon)]\rangle. \tag{21}$$

The currents induced by $\delta\mathbf{A}(\mathbf{R};t)$ can then be calculated directly from the Keldysh propagator $\delta\hat{g}^K$ via

$$\delta\mathbf{j}(\mathbf{R};t)=eN_f\int\frac{d\epsilon}{4\pi i}\langle\mathbf{v}_f(\mathbf{p}_f')\mathrm{Tr}[\hat{\tau}_3\delta\hat{g}^K(\mathbf{p}_f',\mathbf{R};\epsilon,t)]\rangle. \tag{22}$$

The external field also induces nonequilibrium thermal currents in the vortex core, which are given by

$$\delta\mathbf{j}_\varepsilon(\mathbf{R};t)=N_f\int\frac{d\epsilon}{4\pi i}\langle\epsilon\mathbf{v}_f(\mathbf{p}_f')\mathrm{Tr}[\hat{\tau}_0\delta\hat{g}^K(\mathbf{p}_f',\mathbf{R};\epsilon,t)]\rangle - \mathbf{j}_0(\mathbf{R})\,\delta\Phi(\mathbf{R};t). \tag{23}$$

The self-consistent solution of the quasiclassical equations ensure the following conservation laws for charge and energy:

$$\partial_t\delta\rho^{(1)}(\mathbf{R};t)+\boldsymbol{\nabla}\cdot\delta\mathbf{j}(\mathbf{R};t)=0, \tag{24}$$

$$\partial_t\delta\varepsilon(\mathbf{R};t)+\boldsymbol{\nabla}\cdot\delta\mathbf{j}_\varepsilon(\mathbf{R};t)=\mathbf{j}_0(\mathbf{R})\cdot\delta\mathbf{E}(\mathbf{R};t), \tag{25}$$

where $\delta\varepsilon(\mathbf{R};t)$ is a local energy density, and $\delta\mathbf{E}(\mathbf{R};t)=\delta\mathbf{E}_0^\omega(t)-\boldsymbol{\nabla}\delta\Phi(\mathbf{R};t)$ is the total electric field. Because of the local charge neutrality condition (19), the first equation reduces to $\boldsymbol{\nabla}\cdot\delta\mathbf{j}(\mathbf{R};t)=0$.

B. Scalar transport equations

The numerical solution of nonequilibrium transport problems is greatly simplified by a reformulation of the nonequilibrium quasiclassical equations.[12] For a derivation of these equations from the standard equations listed above we use the projection operators introduced by Shelankov,[13]

$$\hat{P}_+^{R,A}=\frac{1}{2}\left(\hat{1}+\frac{1}{-i\pi}\hat{g}_0^{R,A}\right),\quad \hat{P}_-^{R,A}=\frac{1}{2}\left(\hat{1}-\frac{1}{-i\pi}\hat{g}_0^{R,A}\right). \tag{26}$$

The projection operators obey the algebraic relations that follow from the normalization conditions (11),

$$(\hat{P}_+^{R,A})^2=\hat{P}_+^{R,A},\quad (\hat{P}_-^{R,A})^2=\hat{P}_-^{R,A},$$
$$\hat{P}_+^{R,A}\hat{P}_-^{R,A}=\hat{P}_-^{R,A}\hat{P}_+^{R,A}=0. \tag{27}$$

We use the following convenient parametrization of the equilibrium propagators,[14]

$$\hat{g}_0^{R,A}=\mp i\pi N_0^{R,A}\begin{pmatrix}1-\gamma_0^{R,A}\tilde{\gamma}_0^{R,A} & 2\gamma_0^{R,A}\\ 2\tilde{\gamma}_0^{R,A} & -1+\gamma_0^{R,A}\tilde{\gamma}_0^{R,A}\end{pmatrix}, \tag{28}$$

$$\hat{g}_0^K=(\hat{g}_0^R-\hat{g}_0^A)\tanh(\epsilon/2T), \tag{29}$$

$$N_0^{R,A}=\frac{1}{1+\gamma_0^{R,A}\tilde{\gamma}_0^{R,A}}, \tag{30}$$

where the scalar functions $\gamma_0^{R,A}$ are obtained by solving the Riccati type transport equations

$$i\mathbf{v}_f\cdot\boldsymbol{\nabla}\gamma_0^{R,A}+2\epsilon\gamma_0^{R,A}=-\tilde{\Delta}^{R,A}(\gamma_0^{R,A})^2+2\Sigma^{R,A}\gamma_0^{R,A}-\Delta^{R,A}, \tag{31}$$

$$i\mathbf{v}_f\cdot\boldsymbol{\nabla}\tilde{\gamma}_0^{R,A}-2\epsilon\tilde{\gamma}_0^{R,A}=-\Delta^{R,A}(\tilde{\gamma}_0^{R,A})^2-2\tilde{\Sigma}^{R,A}\tilde{\gamma}_0^{R,A}-\tilde{\Delta}^{R,A}. \tag{32}$$

Unphysical solutions are eliminated by choosing initial conditions properly. The initial conditions for γ_0^R and $\tilde{\gamma}_0^A$ have to be chosen so that their transport equations are stable in direction of $\mathbf{v}_f$, and the initial conditions for $\tilde{\gamma}_0^R$ and γ_0^A so that their transport equations are stable in direction of $-\mathbf{v}_f$. We use the following short-hand notation for the driving terms in the transport equations:

$$\hat{\Delta}_{mf0}^{R,A}+\hat{\sigma}_{i0}^{R,A}-\frac{e}{c}\mathbf{v}_f\cdot\mathbf{A}\hat{\tau}_3=\begin{pmatrix}\Sigma^{R,A} & \Delta^{R,A}\\ -\tilde{\Delta}^{R,A} & \tilde{\Sigma}^{R,A}\end{pmatrix}, \tag{33}$$

$$\delta\check{h}=\delta\check{\Delta}_{mf}+\delta\check{\sigma}_i+\delta\check{v},$$

$$\delta\hat{h}^K=\delta\hat{h}^R\otimes\tanh(\beta\epsilon/2)-\tanh(\beta\epsilon/2)\otimes\delta\hat{h}^A+\delta\hat{h}^a,$$

$$\delta\hat{h}^{R,A}=\begin{pmatrix}\delta\Sigma^{R,A} & \delta\Delta^{R,A}\\ -\delta\tilde{\Delta}^{R,A} & \delta\tilde{\Sigma}^{R,A}\end{pmatrix},\quad \delta\hat{h}^a=\begin{pmatrix}\delta\Sigma^a & \delta\Delta^a\\ \delta\tilde{\Delta}^a & -\delta\tilde{\Sigma}^a\end{pmatrix}. \tag{34}$$

The key result is that the Nambu matrices $\delta\hat{g}^{R,A,K}$ can be expressed, with the help of Shelankov's projectors, in terms of six scalar functions, $\delta\gamma^{R,A}$, $\delta\tilde{\gamma}^{R,A}$, δx^a, and $\delta\tilde{x}^a$, each of which is a function of $\mathbf{p}_f$, $\mathbf{R}$, ϵ, t, and satisfies a scalar transport equation. From the first-order normalization conditions (13) we have $\hat{P}_+^{R,A}\otimes\delta\hat{g}^{R,A}\otimes\hat{P}_+^{R,A}=0$ and $\hat{P}_-^{R,A}\otimes\delta\hat{g}^{R,A}\otimes\hat{P}_-^{R,A}=0$; as a consequence the *spectral response* $\delta\hat{g}^{R,A}$, can be written as

$$\delta\hat{g}^{R,A}=\mp 2\pi i[\hat{P}_+^{R,A}\otimes\delta\hat{X}^{R,A}\otimes\hat{P}_-^{R,A}-\hat{P}_-^{R,A}\otimes\delta\hat{Y}^{R,A}\otimes\hat{P}_+^{R,A}]. \tag{35}$$

The Nambu matrices $\delta\hat{X}^{R,A}$ and $\delta\hat{Y}^{R,A}$ are not uniquely defined. However, a convenient parametrization in terms of two scalar functions $\delta\gamma^{R,A}$ and $\delta\tilde{\gamma}^{R,A}$ is given by

$$\delta\hat{g}^{R,A}=\mp 2\pi i\left[\hat{P}_+^{R,A}\otimes\begin{pmatrix}0 & \delta\gamma^{R,A}\\ 0 & 0\end{pmatrix}\otimes\hat{P}_-^{R,A} - \hat{P}_-^{R,A}\otimes\begin{pmatrix}0 & 0\\ -\delta\tilde{\gamma}^{R,A} & 0\end{pmatrix}\otimes\hat{P}_+^{R,A}\right]. \tag{36}$$

It is convenient to transform from the Keldysh response function, $\delta\hat{g}^K$ to the *anomalous response* function $\delta\hat{g}^a$

$$\delta\hat{g}^K=\delta\hat{g}^R\otimes\tanh(\epsilon/2T)-\tanh(\epsilon/2T)\otimes\delta\hat{g}^A+\delta\hat{g}^a. \tag{37}$$

The normalization condition (13) gives $\hat{P}_+^R\otimes\delta\hat{g}^a\otimes\hat{P}_+^A=0$ and $\hat{P}_-^R\otimes\delta\hat{g}^a\otimes\hat{P}_-^A=0$, so that $\delta\hat{g}^a$ can be written in the following form:

$$\delta\hat{g}^a=-2\pi i[\hat{P}_+^R\otimes\delta\hat{X}^a\otimes\hat{P}_-^A+\hat{P}_-^R\otimes\delta\hat{Y}^a\otimes\hat{P}_+^A], \tag{38}$$

where the freedom in choosing $\delta\hat{X}^a$ and $\delta\hat{Y}^a$ allows us to parametrize $\delta\hat{g}^a$ in terms of two scalar distribution functions δx^a and $\delta\tilde{x}^a$,

$$\delta\hat{g}^a=-2\pi i\left[\hat{P}_+^R\otimes\begin{pmatrix}\delta x^a & 0\\ 0 & 0\end{pmatrix}\otimes\hat{P}_-^A + \hat{P}_-^R\otimes\begin{pmatrix}0 & 0\\ 0 & \delta\tilde{x}^a\end{pmatrix}\otimes\hat{P}_+^A\right]. \tag{39}$$

The transport equations for the scalar functions $\delta\gamma^{R,A}$, $\delta\tilde{\gamma}^{R,A}$, δx^a, $\delta\tilde{x}^a$ follow from Eqs. (10) and (12). They decouple for given self-energies, and one finds[12] the following set of linearized transport equations:

$$i\mathbf{v}_f\cdot\nabla\delta\gamma^{R,A}+2\epsilon\delta\gamma^{R,A}+(\gamma_0^{R,A}\tilde{\Delta}^{R,A}-\Sigma^{R,A})\otimes\delta\gamma^{R,A}+\delta\gamma^{R,A}\otimes(\tilde{\Delta}^{R,A}\gamma_0^{R,A}+\tilde{\Sigma}^{R,A}) = -\gamma_0^{R,A}\otimes\delta\tilde{\Delta}^{R,A}\otimes\gamma_0^{R,A}+\delta\Sigma^{R,A}\otimes\gamma_0^{R,A}-\gamma_0^{R,A}\otimes\delta\tilde{\Sigma}^{R,A}-\delta\Delta^{R,A}, \tag{40}$$

$$i\mathbf{v}_f\cdot\nabla\delta\tilde{\gamma}^{R,A}-2\epsilon\delta\tilde{\gamma}^{R,A}+(\tilde{\gamma}_0^{R,A}\Delta^{R,A}-\tilde{\Sigma}^{R,A})\otimes\delta\tilde{\gamma}^{R,A}+\delta\tilde{\gamma}^{R,A}\otimes(\Delta^{R,A}\tilde{\gamma}_0^{R,A}+\Sigma^{R,A}) = -\tilde{\gamma}_0^{R,A}\otimes\delta\Delta^{R,A}\otimes\tilde{\gamma}_0^{R,A}+\delta\tilde{\Sigma}^{R,A}\otimes\tilde{\gamma}_0^{R,A}-\tilde{\gamma}_0^{R,A}\otimes\delta\Sigma^{R,A}-\delta\tilde{\Delta}^{R,A}, \tag{41}$$

$$i\mathbf{v}_f\cdot\nabla\delta x^a+i\partial_t\delta x^a+(\gamma_0^R\tilde{\Delta}^R-\Sigma^R)\otimes\delta x^a+\delta x^a\otimes(\Delta^A\tilde{\gamma}^A+\Sigma^A) = \gamma_0^R\otimes\delta\tilde{\Sigma}^a\otimes\tilde{\gamma}_0^A-\delta\Delta^a\otimes\tilde{\gamma}_0^A-\gamma_0^R\otimes\delta\tilde{\Delta}^a-\delta\Sigma^a, \tag{42}$$

$$i\mathbf{v}_f\cdot\nabla\delta\tilde{x}^a-i\partial_t\delta\tilde{x}^a+(\tilde{\gamma}_0^R\Delta^R-\tilde{\Sigma}^R)\otimes\delta\tilde{x}^a+\delta\tilde{x}^a\otimes(\tilde{\Delta}^A\gamma_0^A+\tilde{\Sigma}^A) = \tilde{\gamma}_0^R\otimes\delta\Sigma^a\otimes\gamma_0^A-\delta\tilde{\Delta}^a\otimes\gamma_0^A-\tilde{\gamma}_0^R\otimes\delta\Delta^a-\delta\tilde{\Sigma}^a. \tag{43}$$

The transport equations for $\delta\gamma^R$, $\delta\tilde{\gamma}^A$, δx^a are stable in direction of $\mathbf{v}_f$, and the transport equations for $\delta\tilde{\gamma}^R$, $\delta\gamma^A$, $\delta\tilde{x}^a$ are stable in direction of $-\mathbf{v}_f$.

The linear corrections to the retarded, advanced, and Keldysh Green's function are then given by

$$\delta\hat{g}^{R,A}=\mp 2\pi i N_0^{R,A}\otimes\begin{pmatrix}-(\delta\gamma^{R,A}\otimes\tilde{\gamma}_0^{R,A}+\gamma_0^{R,A}\otimes\delta\tilde{\gamma}^{R,A}) & (\delta\gamma^{R,A}-\gamma_0^{R,A}\otimes\delta\tilde{\gamma}^{R,A}\otimes\gamma_0^{R,A})\\ (\delta\tilde{\gamma}^{R,A}-\tilde{\gamma}_0^{R,A}\otimes\delta\gamma^{R,A}\otimes\tilde{\gamma}_0^{R,A}) & (\delta\tilde{\gamma}^{R,A}\otimes\gamma_0^{R,A}+\tilde{\gamma}_0^{R,A}\otimes\delta\gamma^{R,A})\end{pmatrix}\otimes N_0^{R,A}, \tag{44}$$

$$\delta\hat{g}^a=-2\pi i N_0^R\otimes\begin{pmatrix}(\delta x^a+\gamma_0^R\otimes\delta\tilde{x}^a\otimes\tilde{\gamma}_0^A) & -(\gamma_0^R\otimes\delta\tilde{x}^a-\delta x^a\otimes\gamma_0^A)\\ (\tilde{\gamma}_0^R\otimes\delta x^a-\delta\tilde{x}^a\otimes\tilde{\gamma}_0^A) & (\delta\tilde{x}^a+\tilde{\gamma}_0^R\otimes\delta x^a\otimes\gamma_0^A)\end{pmatrix}\otimes N_0^A. \tag{45}$$

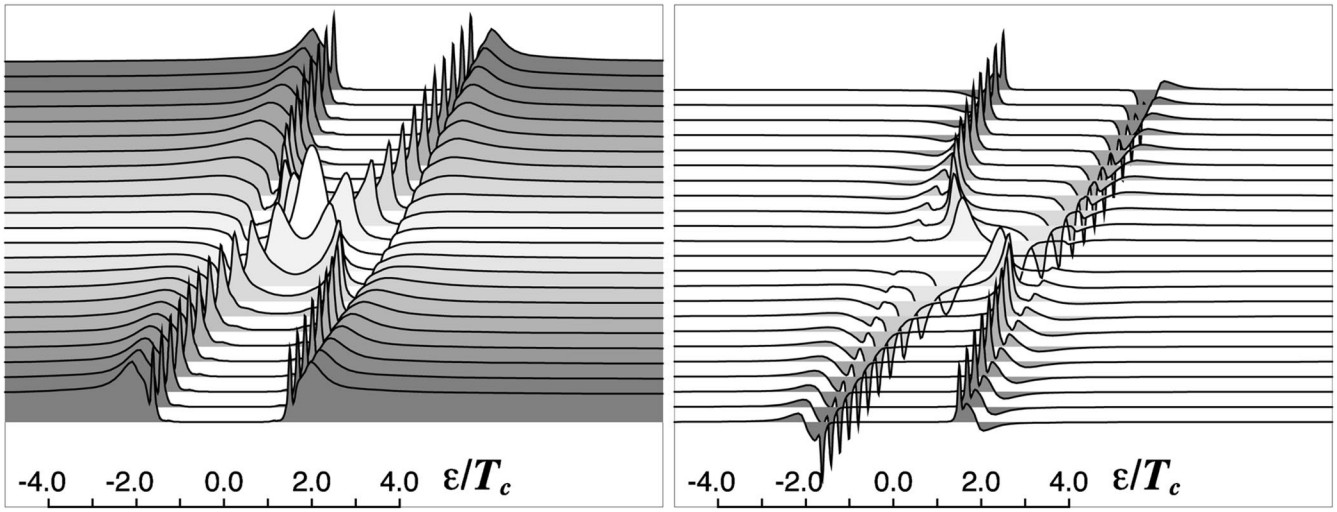

FIG. 1. The left panel shows the local density of states in the core of a vortex as function of energy (ϵ) at different points on a straight line through the vortex center. The spacing of the points is in steps of $0.8\xi_0$, and the largest distance from the center is $8.8\xi_0$. The center of the vortex corresponds to the bright filled spectrum. The right panel is the local spectral current density for the same set of trajectories. Note that the spectral current density is dominated by the current carried by the bound states.

After Fourier transforming Eqs. (40)–(43) we are left with six ordinary differential equations along straight trajectories in R space. The $\otimes$ product is especially simple for the case of linear response. The products are here of the type $\hat{E}\otimes\delta\hat{X}$ or $\delta\hat{X}\otimes\hat{E}$ where $\hat{E}$ is an equilibrium quantity and $\delta\hat{X}$ a response term. In Fourier space one obtains in this case

$$\hat{E}(\epsilon)\otimes\delta\hat{X}(\epsilon,\omega)=\hat{E}(\epsilon+\omega/2)\,\delta\hat{X}(\epsilon,\omega),$$

$$\delta\hat{X}(\epsilon,\omega)\otimes\hat{E}(\epsilon)=\delta\hat{X}(\epsilon,\omega)\hat{E}(\epsilon-\omega/2). \tag{46}$$

For given self-energies, Eqs. (40)–(43) are a *decoupled* set of linear differential equations for the scalar functions, $\delta\gamma^{R,A}$, $\delta\tilde{\gamma}^{R,A}$, δx^a, $\delta\tilde{x}^a$. The solution of this initial value problem is obtained numerically by standard Runge-Kutta methods. This method is superior to the direct solution of the matrix differential equation system, Eqs. (12),(13) (a stiff boundary value problem) which suffers from numerical instabilities and is not as fast. The scalar functions $\delta\gamma^{R,A}$, $\delta\tilde{\gamma}^{R,A}$, δx^a, $\delta\tilde{x}^a$, are coupled through the self-consistency conditions for $\delta\Delta^{R,A,a}$ and $\delta\Sigma^{R,A,a}$, which determine the right-hand sides of Eqs. (40)–(43). The self-consistency problem is solved numerically in an effective way using special algorithms for updating the right-hand side of Eqs. (40)–(43).[12]

III. RESULTS AND DISCUSSION

The linear response equations require as input the self-consistent equilibrium functions $\gamma_0^{R,A}$, $\tilde{\gamma}_0^{R,A}$, and equilibrium self-energies $\Sigma^{R,A}$, $\tilde{\Sigma}^{R,A}$, $\tilde{\Delta}^{R,A}$, $\tilde{\Delta}^{R,A}$. They are obtained by solving Eqs. (31),(32) self-consistently with Eqs. (14) and (16), using Eqs. (28)–(30) and (33). Given these solutions we then solve the first-order transport equations (40)–(43) together with the linearized self-energy equations (15),(17) and the charge neutrality condition (19), using the relations (44)–(46), (37), and (34). The linear response limit is valid as long as the expansion parameter δ is small enough; where $\delta=e|\delta\mathbf{E}_0|\xi_0\Delta/\omega^2$ for $\omega\gtrsim 1/\tau$, $\delta=e|\delta\mathbf{E}_0|\xi_0\Delta\tau/\omega$ for $\omega\lesssim 1/\tau$, and $\delta=e|\delta\mathbf{E}_0|\xi_0/\omega$ for $\omega\gtrsim\Delta$. In these cases the changes $\delta\Delta_{mf}$ are small compared to the equilibrium order parameter Δ_{mf0} and the spatial oscillation amplitude of the vortex center (defined as the point where the order parameter vanishes) is small compared to the coherence length.

The calculations are done for layered s-wave superconductors with a cylindrical Fermi surface along the c direction, isotropic Fermi velocity $\mathbf{v}_f$ in the ab plane and a large Ginzburg-Landau parameter $\kappa\gg 1$. Impurity scattering is taken into account self-consistently in the Born approximation. We consider a moderately clean superconductor with a mean free path, $l=10\xi_0$, and choose a low temperature $T=0.3\,T_c$. We present results for s-wave pairing since the dynamics associated with the continuum and bound states is most clearly distinguishable in this case. However, the vortex-core dynamics of a d-wave superconductor[12] is qualitatively similar to the s-wave case presented here.

Figure 1, left panel, shows the calculated local density of states

$$N_0(\mathbf{R},\epsilon)=N_f\frac{1}{4\pi i}\langle\mathrm{Tr}[\hat{\tau}_3\hat{g}_0^A(\mathbf{p}_f',\mathbf{R};\epsilon)-\hat{\tau}_3\hat{g}_0^R(\mathbf{p}_f',\mathbf{R};\epsilon)]\rangle, \tag{47}$$

of an equilibrium vortex at various distances from the core center. The important feature at the vortex center is the zero-energy bound state, which is broadened by impurity scattering into a resonance of width $\Gamma\approx 0.6\,T_c$. At finite distances from the vortex center the bound states of quasiparticles with different angular momenta (different impact parameter) form a one-dimensional band, which is broadened by impurity scattering. The bands widen with increasing distance from the center because of the coupling to the vortex flow field, and develop Van Hove singularities at the band edges. The continuum edges show a characteristic shape as a result of Doppler shifts due to the circulating supercurrents. At the

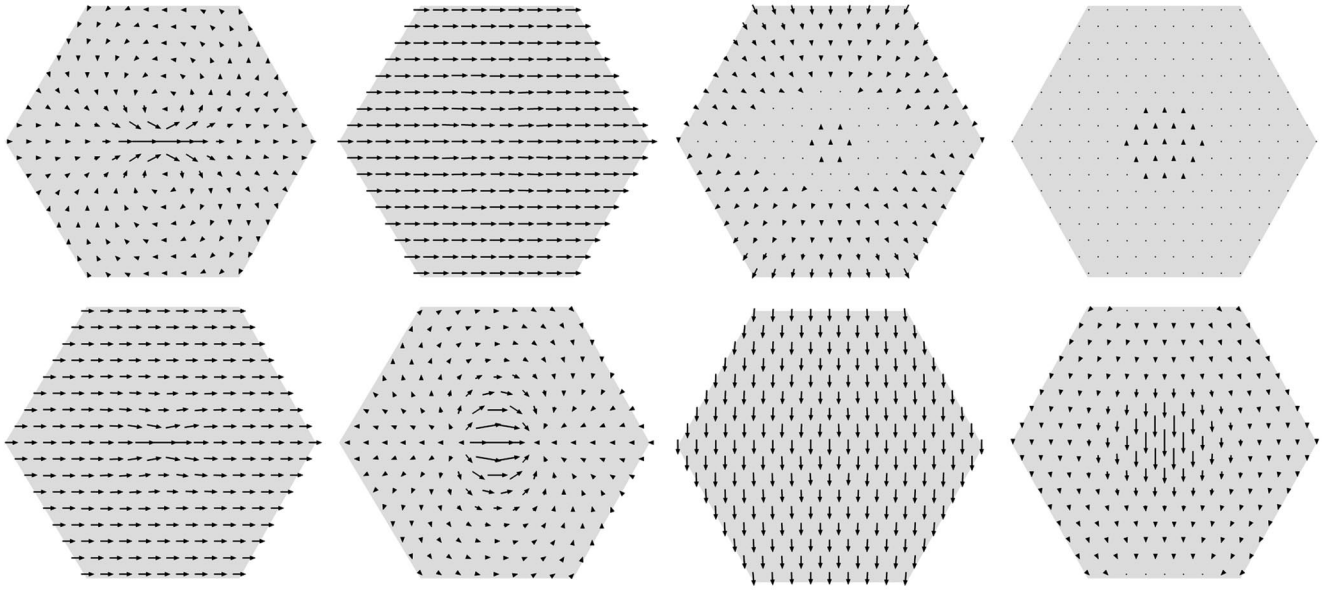

FIG. 2. Two-dimensional plot of the charge current density distribution (first column) and corresponding local (external+induced) electric field (second column). The order parameter displacement velocity field is shown in the third column, and the thermal current density distribution is shown in the fourth column. The results are for a frequency of $\omega=0.3\Delta$ with the external field along the x direction. The top row shows the amplitude of the in-phase response ($\sim\cos\omega t$), while the bottom row shows the reactive response ($\sim\sin\omega t$). Distances from the vortex center extend up to $6.3\xi_0$.

vortex center, as a result of self-consistency, there is no enhancement of the density of states at the continuum edge. The right panel of Fig. 1 is the corresponding spectral current density[4]

$$\mathbf{j}_0(\mathbf{R},\epsilon)=2eN_f\frac{1}{4\pi i}\langle\mathbf{v}_f(\mathbf{p}_f')\mathrm{Tr}[\hat{\tau}_3\hat{g}_0^A(\mathbf{p}_f',\mathbf{R};\epsilon)-\hat{\tau}_3\hat{g}_0^R(\mathbf{p}_f',\mathbf{R};\epsilon)]\rangle, \tag{48}$$

for the vortex as a function of the impact parameter, which illustrates clearly that the equilibrium current density in the core of the vortex is carried by the bound states.

The first two columns in Fig. 2 show typical results for the current patterns $\delta\mathbf{j}(\mathbf{R},t)$ and field patterns $\delta\mathbf{E}(\mathbf{R},t)$, induced by an external electric field of the form $\delta\mathbf{E}_0^\omega(t)=\delta\mathbf{E}_0\cos(\omega t)$. The system responds with an in-phase response [$\sim\cos(\omega t)$] and out-of-phase response [$\sim\sin(\omega t)$]. The in-phase current response at position $\mathbf{R}$ determines the local time-averaged energy transfer between the external field and the electrons, $\mathcal{E}(\mathbf{R})=\langle\delta\mathbf{j}(\mathbf{R},t)\cdot\delta\mathbf{E}_0^\omega(t)\rangle_t$, while the out-of-phase current response is non-dissipative. Absorptive and reactive currents show characteristically different flow patterns. The nondissipative current response, $\delta\mathbf{j}''$, is nearly homogeneous (see lower left pattern of Fig. 2), whereas the pattern of absorptive current response $\delta\mathbf{j}'$, has qualitatively the form of a vortex-antivortex pair (see upper left pattern of Fig. 2). Hence, the part $\mathbf{j}_0+\delta\mathbf{j}'$ of the total current density $\mathbf{j}_0+\delta\mathbf{j}$, describes a transverse oscillation of the equilibrium current pattern in the y direction. The amplitude of this oscillation increases with decreasing frequency. At higher frequency the current pattern deviates significantly from a rigid shift, as can be seen in Fig. 5 (discussed below). The second column of Fig. 2 shows the total electric field, $\delta\mathbf{E}(\mathbf{R},t)=\delta\mathbf{E}_0^\omega(t)-\boldsymbol{\nabla}\delta\Phi(\mathbf{R},t)$, which consists of the homogeneous external field and the internal field due to charge fluctuations induced by the external field. Note that the induced field is predominantly out-of-phase and exceeds the external field in the center of the vortex core. For higher frequencies, $0.5\Delta\lesssim\omega\lesssim2\Delta$, the induced dipolar field evolves from an out-of-phase dipolar field along the direction of the applied field to an in-phase dipolar field opposite to the applied field, thus reducing the external field by roughly one half. The induced field vanishes rapidly for frequencies above the gap edge. The charge density fluctuations responsible for the induced field $\delta\rho(\mathbf{R},t)=-\boldsymbol{\nabla}^2\delta\Phi(\mathbf{R},t)$, are of the order $(e\delta/\xi_0^2)\cdot(\Delta/E_f)$. Thus, only a fraction $(e\delta)\cdot(\Delta/E_f)$ of an elementary charge oscillates periodically in time over an area of ξ_0^2. The charge accumulation is consistent with the condition of local charge neutrality,[10] as discussed in Sec. II A. We note that the induced charge in the vortex core resulting from particle-hole asymmetry, as discussed recently,[15] is of order $e(\Delta/E_f)^2$, i.e., of second order in Δ/E_f and negligible in the context of this paper. However, the particle-hole asymmetric charges give a comparable contribution to the dynamics of the vortex core for sufficiently small excitation fields, i.e., $\delta\sim\Delta/E_f$, which may be relevant in high-T_c superconductors.

The in-phase current and field response (upper row of Fig. 2) imply that the local absorption can be either positive [''hot spots'' with $\mathcal{E}(\mathbf{R})>0$ in the vortex center], or negative [''cold spots'' with $\mathcal{E}(\mathbf{R})<0$ above and below the vortex center], and is dominated by the absorption in the vortex center. The net dissipation is positive, and is obtained by integrating $\mathcal{E}(\mathbf{R})$ over the vortex. At higher frequencies the dissipation is dominated by higher energy bound states and is located away from the vortex center (see Fig. 5).

The electromagnetic response of the vortex core is due to an interplay between collective dynamics of the order param-

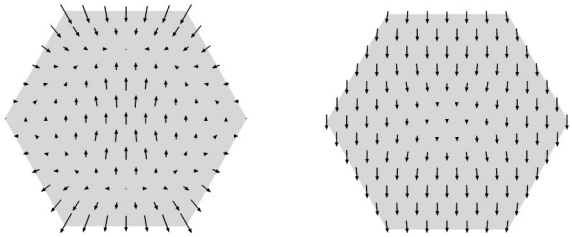

FIG. 3. The order parameter displacement velocity for an applied electric field with $\omega = 1.2\Delta$. The difference in the velocities at the inner and outer region of the core is indicative of strong order parameter deformation. The left panel shows the in-phase velocity field, and the right panel the out-of-phase velocity field. Distances from the center of the core extend up to $4.7\xi_0$.

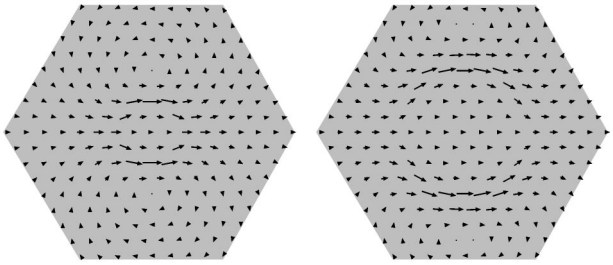

FIG. 5. Dissipative currents in the vortex core induced by an external electric field in the x direction with $\omega = 1.1\Delta$ (left) and 1.5Δ (right). Note that the current density at $\omega = 1.5\Delta$ is scaled by a factor 2.5 relative to the current density at 1.1Δ. Distances from the center extend up to $6.3\xi_0$.

eter and the dynamics of the Caroli–de Gennes–Matricon bound states. We find that at low frequencies, $\omega \approx 1/\tau$, the order parameter performs a nearly homogeneous oscillation perpendicular to the applied field, with a velocity that is 90° out of phase with the applied field. To analyze the deviations of the self-consistent order parameter from the rigidly moving vortex structures for $\omega \ll \Delta_{mf}$ we introduce the order parameter displacement vector $\delta\mathbf{R}_0(t)$ defined by $\delta\Delta(\mathbf{R},t) = \delta\mathbf{R}_0(\mathbf{R},t)\cdot\nabla\Delta_{mf0}(\mathbf{R})$. The velocity field of the order parameter is then $\delta\mathbf{v}(\mathbf{R},t) = \partial_t\delta\mathbf{R}_0(\mathbf{R},t)$. The nearly homogeneous oscillation at low frequencies is shown in Fig. 2 for $\omega = 0.3\Delta$ in the third column. The order parameter velocity field for a higher frequency $\omega = 1.2\Delta$, is shown in Fig. 3. The vortex core oscillates at these frequencies in-phase and perpendicular to the applied field but is strongly deformed. In one period the vortex center moves a distance of order of the coherence length multiplied with the linear-response expansion parameter δ. So, the velocity of the vortex center is of the order of $\xi_0\omega\delta \sim v_f\delta$. Nevertheless, the current density in the vortex core is smaller by a factor δ compared to the Landau critical current density. For $\omega \gtrsim \Delta$, both the phase and amplitude of the vortex core oscillation decrease and approach zero above $\omega \sim 2\Delta$. In Fig. 2, last column, we show the energy current density, $\delta\mathbf{j}_\varepsilon(\mathbf{R},t)$, for $\omega = 0.3\Delta$. Our calculations show that the energy flow in the vortex core is predominantly in direction of the order parameter oscillation and is restricted to the core region.

The coupling between order parameter response and the bound states is demonstrated in Fig. 4, which compares the

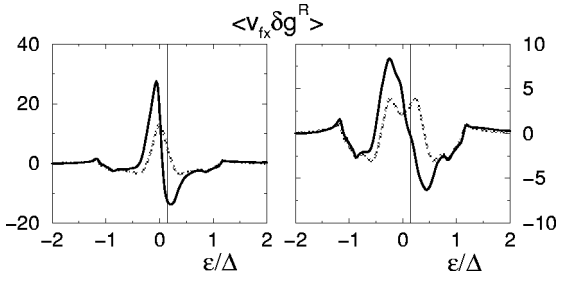

FIG. 4. Absorptive part of the spectral current density $\langle v_{fx}\delta g^R(\mathbf{p}_f,\mathbf{R};\epsilon)\rangle$, at the vortex center (left) and at point $(0.8\xi_0,0)$ on the x axis (right) for $\omega = 0.3\Delta$. The vertical lines denote $\epsilon = \omega/2$. The solid curves are the fully self-consistent spectral response, while the dashed lines represent the spectrum for a frozen order parameter.

absorptive part of the nonequilibrium spectral current density $\delta j_x^S(\epsilon) = \langle v_{fx}\,\mathrm{Tr}[\hat{\tau}_3\delta\hat{g}^R(\mathbf{p}_f';\epsilon)]\rangle$, obtained from a self-consistent calculation with that obtained from a non-self-consistent calculation that takes into account the field-induced transitions within the band of Caroli–de Gennes–Matricon bound states, but freezes the order parameter degrees of freedom. The corresponding contribution to the current density is obtained by multiplying these functions by the Fermi function centered at $\epsilon = \omega/2$, and integrating over ϵ:[16] $\delta j_x^S = \int (d\epsilon/\pi)\, f(\epsilon - \omega/2)\,\delta j_x^S(\epsilon)$. The absorptive part of the response function shows peaks in the spectral current density associated with the band of bound states in the vortex core. The spectral weight above $\epsilon = \omega/2$ does not contribute significantly to the current response. Figure 4 shows that the bound state band is shifted to lower energy by the self-consistent response of the order parameter, leading to a strong enhancement of the absorptive current.

The absorptive currents show a nontrivial structure for frequencies in the range $\Delta < \omega < 2\Delta$. Figure 5 shows that the absorptive currents flow predominantly in regions where bound states with energy $\epsilon_{bs} = \omega/2$ are localized. We interpret these structures in terms of impurity-mediated transitions between the Van Hove band edges (shown in Fig. 1) of the bound-state bands of the equilibrium vortex. The transition rate increases with decreasing frequency, and for ω comparable to the width of the zero energy resonance in the bound state spectrum the absorption is determined by the spectral dynamics of the zero energy resonance at the vortex center. The spectral response of these states (Fig. 4) leads to a dramatically enhanced absorption near the vortex center, which is much larger than in the normal state.

It is convenient to describe the response of an inhomogeneous system to a homogeneous electric field by a ''local conductivity,'' $\sigma_{ij}(\mathbf{R},\omega)$. It is defined by the linear relation, $\delta j_i(\mathbf{R},\omega) = \sigma_{ij}(\mathbf{R},\omega)\,\delta E_{0j}(\omega)$, between the current density, $\mathbf{j}(\mathbf{R},\omega)$, and the amplitude of the homogeneous field, $\delta\mathbf{E}_0(\omega)$. Figure 6 shows the local conductivity in the vicinity of the vortex core as a function of frequency for various distances from the vortex center. At the vortex center the real part of σ_{xx} (absorption) increases rapidly at low frequencies. Further away from the center the absorption has a maximum at a frequency corresponding to transitions between states near the Van Hove peaks of the bound state band. For comparison we show in Fig. 6 the conductivity of a homogeneous superconductor with the same mean-free path. It

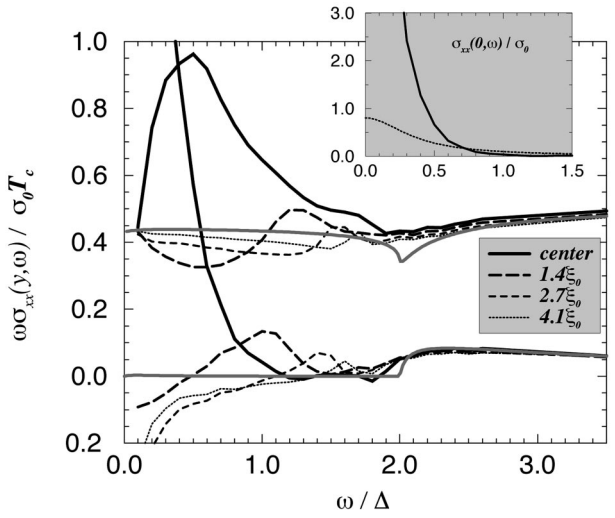

FIG. 6. Local conductivity in the vortex core as a function of frequency. The lower set of curves show $\omega\,\mathrm{Re}\,\sigma_{xx}$ as a function of distance from the center (shown in the legend) along the $\hat{\mathbf{y}}$ direction. The upper set of curves are $\omega\,\mathrm{Im}\,\sigma_{xx}$. The thick black curves correspond to the vortex center. For comparison, the thick gray curves are the conductivity for a homogeneous superconductor with the same mean-free-path, which illustrates the role of the vortex-core bound states in the EM response of the core. The inset shows a comparison of the Drude absorption (dotted curve) of a normal metal with the enhanced absorption at the center of the vortex core (full curve). Note that $\sigma_0=2e^2N_fv_f^2$, $l=10\xi_0$ and $T=0.3T_c$.

shows the typical absorption edge for s-wave pairing at $\omega=2\Delta$. It should be emphasized that the low-frequency absorption in the vortex center is much larger than the Drude absorption in the normal state (inset of Fig. 6). This effect reflects the existence of the zero-energy resonance in the bound state spectrum at the vortex center (see Fig. 1). The conductivity sum-rule is obeyed despite this enhanced absorption. The apparent excess weight of $\int \mathrm{Re}\,\sigma_{xx}(\omega)d\omega$ is compensated by a negative δ function contribution associated with counterflowing supercurrents near the vortex center. Figure 6 also shows enhanced supercurrents in the vortex center (as compared to a homogeneous superconductor) for frequencies comparable with the width of the zero-energy resonance.

Finally we note that the order parameter response at low frequencies is mostly transverse to the electric field and that the absorptive current in the core is predominantly parallel to the applied field, i.e., there are no charge currents in the y direction related to the order parameter motion. However, there is a substantial energy flow in the y direction. Our calculations show that the energy flow in the vortex core is predominantly in direction of the order parameter oscillation and transports energy from ''hot spots'' to ''cold spots.'' Thus, the states in the vortex core extract energy from the external field, and transport this energy several coherence lengths away from the vortex center in the y direction. The net dissipation will finally be determined by inelastic processes in the vortex core.

ACKNOWLEDGMENTS

We acklowledge helpful discussions with F. Marquardt, A. H. MacDonald, and W. A. Atkinson. The work of M.E. and J.A.S. was supported partly by the STCS through NSF Grant No. 91-20000, M.E. and D.R. were supported partly by the Deutsche Forschungsgemeinschaft, and D.R. and J.A.S. also acknowledge support from the Max-Planck-Gesellschaft and the Alexander von Humboldt-Stiftung.

[1] J. Bardeen and M. J. Stephen, Phys. Rev. **140**, A1197 (1965).
[2] C. Caroli, P.-G. de Gennes, and J. Matricon, Phys. Lett. **9**, 307 (1964).
[3] J. Bardeen, R. Kümmel, A. E. Jacobs, and L. Tewordt, Phys. Rev. **187**, 556 (1969).
[4] D. Rainer, J. A. Sauls, and D. Waxman, Phys. Rev. B **54**, 10 094 (1996).
[5] B. Jankó and J. D. Shore, Phys. Rev. B **46**, 9270 (1992); T. C. Hsu, Physica C **213**, 305 (1993); H. D. Drew and T. C. Hsu, Phys. Rev. B **52**, 9178 (1995); Y.-D. Zhu, F.-C. Zhang, and H. D. Drew, *ibid.* **47**, 586 (1993).
[6] N. B. Kopnin, JETP Lett. **27**, 391 (1978); N. B. Kopnin and A. V. Lopatin, Phys. Rev. B **51**, 15 291 (1995); N. B. Kopnin and G. E. Volovik, Phys. Rev. Lett. **79**, 1377 (1997); N. B. Kopnin, Phys. Rev. B **57**, 11 775 (1998).
[7] The ac vortex core response, restricted to superclean limit, was recently discussed by W. A. Atkinson and A. H. MacDonald, Phys. Rev. B **60**, 9295 (1999); and by A. A. Koulakov and A. I. Larkin, Phys. Rev. B **59**, 12 021 (1999).
[8] G. Eilenberger, Z. Phys. **214**, 195 (1968); A. I. Larkin and Y. N. Ovchinnikov, Sov. Phys. JETP **28**, 1200 (1969); **41**, 960 (1976); **46**, 155 (1977); G. M. Eliashberg, *ibid.* **34**, 668 (1972).
[9] A. I. Larkin and Y. N. Ovchinnikov, in *Nonequilibrium Superconductivity*, edited by D. N. Langenberg and A. I. Larkin (Elsevier, Amsterdam, 1986), p. 493.
[10] L. P. Gorkov and N. B. Kopnin, Sov. Phys. Usp. **18**, 496 (1975); S. N. Artemenko and A. F. Volkov, *ibid.* **22**, 295 (1979).
[11] J. W. Serene and D. Rainer, Phys. Rep. **101**, 221 (1983).
[12] M. Eschrig, Ph.D. thesis, Bayreuth University, 1997; cond-mat/9804330 (unpublished).
[13] A. L. Shelankov, J. Low Temp. Phys. **60**, 29 (1985).
[14] Y. Nagato, K. Nagai, and J. Hara, J. Low Temp. Phys. **93**, 33 (1993); N. Schopohl and K. Maki, Phys. Rev. B **52**, 490 (1995).
[15] D. I. Khomskii and A. Freimuth, Phys. Rev. Lett. **75**, 1384 (1995); M. V. Feigel'man, V. B. Geshkenbein, A. I. Larkin, and V. M. Vinokur, Pis'ma Zh. Eksp. Teor. Fiz. **62**, 811 (1995) [JETP Lett. **62**, 834 (1995)]; G. Blatter, M. Feigel'man, V. Geshkenbein, A. Larkin, and A. van Otterlo, Phys. Rev. Lett. **77**, 566 (1996).
[16] There is a second contribution to the current density from the ''anomalous'' Green's function. The spectral response shown in Fig. 3 dominates the dissipative current density in the core, while the anomalous response contributes primarily to the reactive response at low frequencies.